

Journal of Biomedical Optics

BiomedicalOptics.SPIEDigitalLibrary.org

Confocal Raman microscopy to monitor extracellular matrix during dental pulp stem cells differentiation

Hamideh Salehi
Pierre-Yves Collart-Dutilleul
Csilla Gergely
Frédéric J. G. Cuisinier

Confocal Raman microscopy to monitor extracellular matrix during dental pulp stem cells differentiation

Hamideh Salehi,^{a,*} Pierre-Yves Collart-Dutilleul,^a Csilla Gergely,^b and Frédéric J. G. Cuisinier^a

^aUniversité de Montpellier, Laboratoire Bioingénierie et Nanoscience (LBN), EA 4203, Avenue du Professeur Jean Louis Viala, Montpellier 34193, France

^bUniversité de Montpellier, Laboratoire Charles Coulomb (L2C), UMR 5221 CNRS, Place Eugène Bataillon, Montpellier 34095, France

Abstract. Regenerative medicine brings promising applications for mesenchymal stem cells, such as dental pulp stem cells (DPSCs). Confocal Raman microscopy, a noninvasive technique, is used to study osteogenic differentiation of DPSCs. Integrated Raman intensities in the 2800 to 3000 cm^{-1} region (C-H stretching) and the 960 cm^{-1} peak (ν_1 PO_4^{3-}) were collected (to image cells and phosphate, respectively), and the ratio of two peaks 1660 over 1690 cm^{-1} (amide I bands) to measure the collagen cross-linking has been calculated. Raman spectra of DPSCs after 21 days differentiation reveal several phosphate peaks: ν_1 (first stretching mode) at 960 cm^{-1} , ν_2 at 430 cm^{-1} , and ν_4 at 585 cm^{-1} and collagen cross-linking can also be calculated. Confocal Raman microscopy enables monitoring osteogenic differentiation *in vitro* and can be a credible tool for clinical stem cell based research. © 2015 Society of Photo-Optical Instrumentation Engineers (SPIE) [DOI: [10.1117/1.JBO.20.7.076013](https://doi.org/10.1117/1.JBO.20.7.076013)]

Keywords: dental pulp stem cells; Raman microscopy; differentiation; collagen cross-link; living cell.

Paper 150171PRRR received Mar. 18, 2015; accepted for publication Jun. 29, 2015; published online Jul. 27, 2015.

1 Introduction

Regenerative medicine aims to restore the normal function of injured tissues by means of cells and scaffolds.¹ Mesenchymal stem cells found in various niches within the human body represent an interesting cell source for cell-based regenerative therapies as they have the ability to self-renew and differentiate into multiple tissues.² Among these, dental pulp stem cells (DPSCs) have been shown to have the potential to differentiate in multiple lineages with a high proliferation rate.³ Dental pulp can be easily collected from teeth after dental extraction. The most frequent case is the collection of normal human wisdom teeth extracted for orthodontic reasons.⁴ A key factor for therapeutic applications using mesenchymal stem cells is to control and follow cell differentiation in order to graft cells that are able to produce a specific tissue. Collagen is a basic component of organic matrix in bone and dentin. Of the total bone protein, 85 to 90% consist of type I collagen, and collagen cross-linking is one of its most distinct features. The collagen network has a significant effect on the mechanical integrity of bone: when collagen is less cross-linked, the bone loses its stiffness.⁵ Monitoring cells' differentiation via the determination of calcium phosphate accumulation and collagen cross-link is possible via confocal Raman microscopy that has been widely used for cell imaging and biological conformation imaging.^{6,7} Each individual conformation (sheets, helices, and so forth) has its specific chemical formulation and, consequently, generates a specific Raman signal. The Raman spectra of individual cells are very complex, and cells spectra^{8,9} and the Raman fingerprints of diverse molecular structures and chemical compounds have been reported previously.¹⁰ High spatial resolution (spatial resolution of 300 nm with a 532 nm laser) and a unique

compositional sensitivity are the main advantages of Raman confocal spectroscopy over other spectroscopic methods.¹¹ In this study, confocal Raman microscopy is used to monitor the differentiation of DPSCs into osteoblast-like cells and the process of extracellular matrix maturing. The DPSCs are multipotent and their differentiation into osteoblasts is eminent for their use in bone regeneration.¹⁰ The significant sign of stem cells differentiation into osteoblasts (to be used to engineer bone tissue) is producing calcium phosphate. Therefore, the detection of phosphate seems necessary as an indication of successful differentiation of DPSC into osteoblasts. We use the ratio of two selected amide I bands revealing the collagen cross-linking and the presence of the phosphate peak after three weeks of culturing in osteogenic medium to monitor DPSCs osteogenic differentiation.

2 Material and Method

2.1 Human Dental Pulp Stem Cells

Human impacted third molars extracted for orthodontic reasons were recovered from healthy patients (15 to 18 years old). Written informed consent was obtained from the parents of the patients. This protocol was approved by the local ethical committee (*Comité de Protection des Personnes*, Montpellier Hospital, France). Tooth surfaces are cleaned using 2% chlorhexidine and cut around the cementum–enamel junction using sterilized discs. Teeth are then broken into two pieces to reveal the pulp chamber. The pulp tissue is gently separated from the crown and root and then digested in a solution of 3 mg/mL collagenase type I and 4 mg/mL dispase for 1 h at 37°C. The solution is then filtered through 70 μm Falcon strainers and added to αMEM supplemented with 10% fetal

*Address all correspondence to: Hamideh Salehi, E-mail: s_hamideh@yahoo.com

bovine serum, 100 U/mL penicillin, 100 $\mu\text{g}/\text{mL}$ streptomycin and placed in 75 ml flasks. Cells are incubated for one week at 37°C with 5% CO_2 . Nonadherent cells are removed by a change of medium 24 h after cell seeding. Cells are cultivated 24 h onto polished calcium fluoride (CaF_2) substrates (Crystran Ltd., Dorset, United Kingdom). Before imaging, the cells cultured on CaF_2 substrates were washed three times with phosphate buffered saline (PBS) to remove the culture medium.

2.2 Dental Pulp Stem Cell Characterization

After one week, subconfluent cells were collected and analyzed for minimal criteria to define human mesenchymal stem cells, such as adherence to plastic, expression of cell surface antigens, and ability to differentiate into osteoblasts, adipocytes, and chondroblasts *in vitro*.¹² The antigen profiles of cultured DPSCs were analyzed by detecting the expression of the cell surface markers CD90, CD146, CD117, and CD45 using flow cytometry. CD90 is a widely accepted marker for mesenchymal stem cells, CD146 is a marker expressed in perivascular mesenchymal stem cells, CD117 is the receptor of stem cell factor, and CD45 is a marker of hematopoietic cells, mainly myeloid progenitors.^{13,14} The latter has been used to demonstrate the absence of contamination by CD45+ hematopoietic progenitors. Cells were controlled for pluripotency with *in vitro* osteogenic, adipogenic, and chondrogenic differentiation following a previously described protocol.¹⁵

2.3 Raman Data Acquisition

Raman spectra were collected using a Witec Confocal Raman Microscope System alpha 300R (Witec Inc., Ulm, Germany). Excitation in confocal Raman microscopy is generated by a frequency doubled Nd:YAG laser (Newport, Evry, France) at a wavelength of 532 nm. The incident laser beam is focused onto the sample through a $\times 60$ NIKON water immersion objective having a numerical aperture of 1.0 and a working distance of 2.8 mm (Nikon, Tokyo, Japan). The laser power passing objective is 15 mW, but the absorbed power by cells in PBS is less. The spatial resolution and depth resolution are 300 nm and 1 μm , respectively. The microscope is equipped with a piezo-driven scan-stage with a positioning accuracy of ~ 2 to 3 nm horizontally and 10 nm vertically, respectively. Then Raman backscattered radiation mixed with the Rayleigh scattered radiation were passed through an edge filter to block the Rayleigh signal. The acquisition time of a single spectrum was set to 0.5 s. 150×150 points per image were recorded, leading to a total of 22,500 spectra for one image, each spectrum corresponding to a spatial unit defined as a voxel. Data acquisition is performed using Image Plus 2.08 software from Witec.

2.4 Data Analysis

Data analysis is based on two methods. The first method provides integrated Raman intensities in specific regions, in particular CH and phosphate stretching modes. Data processing is performed using Image Plus software from Witec. Each image composed of integrated intensities provides a colored map of the sample: bright yellow hues indicate the highest intensities while orange hues the lowest integrated intensities of the chosen region.

The second method consists of a graph calculator and an image cross-section realized using the Witec Project Plus

(Ulm, Germany) software. An image obtained with the Witec Project Plus software represents a ratio of two different reconstructed images. Hence, at each pixel, a number with a corresponding color indicates the ratio of those two peaks at a given point of the sample.

In each image, a cross-section is plotted indicating the pixel intensities. This graph could provide selected the pixels' ratio to simplify the data interpretation. More details are presented in Sec. 3.

3 Results

In order to use stem cells in tissue regeneration, monitoring the cells' differentiation and the process of extracellular maturing seems necessary. With this aim, we applied confocal Raman microscopy to evaluate differentiation of DPSCs and extracellular matrix. DPSCs cultured with osteogenic medium were followed weekly, from the first day until day 21. Control experiments without osteogenic medium were also performed (the results are not presented). After 21-day cultivation of DPSCs in osteogenic medium, the phosphate peak appears. Figure 1(a) is a reconstructed Raman image revealing the respective intensities of the stretching mode of CH band (2800 to 3000 cm^{-1}) in red and a phosphate stretching mode ($\nu_1 \text{PO}_4^{3-}$ at 960 cm^{-1}) in green color, respectively. The CH bands allow mapping of intracellular organelles as previously reported.¹⁶ Here, cells are confluent after a 21 day culture; hence, no such details can be observed and the CH band is used to localized cells and organic extracellular matrix. Figure 1(b)

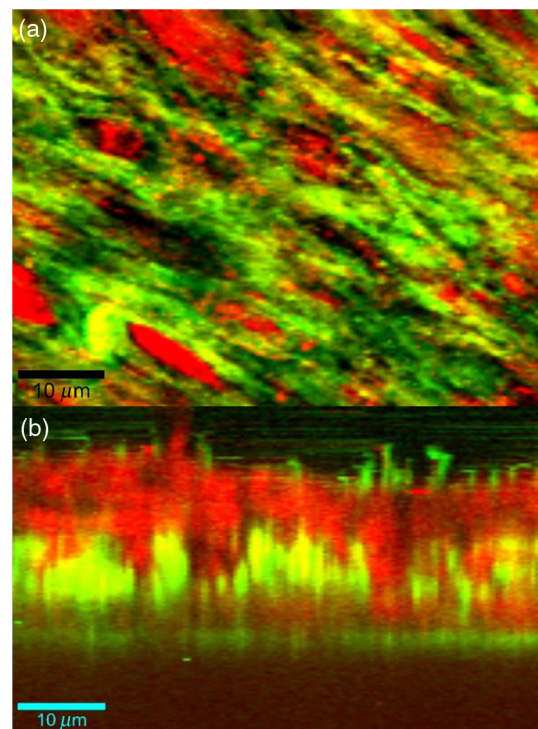


Fig. 1 Dental pulp stem cells (in buffer containing the osteogenic medium) after 21 day culture, 60 \times objective. Reconstructed image obtained using the intensity of specific Raman spectral modes: (a) top and (b) lateral (in-depth) view of the cells: the CH stretching mode (2800 to 3000 cm^{-1}) in red reveals the cells, whereas the green indicates the phosphate stretching mode ($\nu_1 \text{PO}_4^{3-}$ at 960 cm^{-1}). Each pixel is collected at a dwell time of 0.5 s/point and a point spacing of ~ 300 nm.

depicts the reconstructed Raman image obtained after a depth scan, where formation of phosphate in green and organization of cells in red can also be remarked. Phosphates are formed under the cells, and as they are confluent after 14 days of culture and formed a well-packed layer, we can suppose that the phosphate layer between and under the cells is released from cells and does not come from precipitation from the osteogenic medium.

Two typical single spectra selected from cells and the phosphate-rich regions are plotted in Fig. 2: the green spectrum depicts the phosphate-rich region, whereas the red one corresponds to the cell (CH-rich region). Comparing these spectra, we can note three phosphate peaks: ν_1 PO_4^{3-} (first stretching mode) at 960 cm^{-1} , ν_2 PO_4^{3-} at 430 cm^{-1} , and ν_4 PO_4^{3-} at 585 cm^{-1} in the green spectrum that are absent in the red spectrum of the cells. Due to the long time cell culturing, a huge number of cells are present on the substrate; therefore, CH peaks of cell layers on the bottom of the phosphate layer also appear in the phosphate-rich region. Another peak, present only in the green spectrum at 1032 cm^{-1} and coming from the CH_2 CH_3 bending mode of collagen,¹⁷ is absent in the cell spectrum.

As mentioned before, after 21 days of proliferation, a confluent layer of cells was formed, which rendered single cell imaging impossible. To overcome this problem, cells after 21 day culture in osteogenic medium were trypsinized and centrifuged. Treated cells were plated in a Petri dish and allowed to adhere for 24 h on the CaF_2 substrate and then imaged by Raman microscopy. Figure 3 shows a reconstructed Raman image based on the CH stretching mode intensities (2800 to 3000 cm^{-1}). The green cluster presents the position of phosphate in the confocal plane of a single cell. The average spectrum presented in Fig. 3 clearly shows a peak corresponding to the stretching ν_4 mode of phosphate at 960 cm^{-1} .

The spectrum in Fig. 3 also depicts other molecular Raman vibration modes of various cellular components, including phenylalanine at 1004 cm^{-1} , amide I at 1660 cm^{-1} , and carbohydrate CH_2 amide I at 1449 cm^{-1} . The phosphate signal was present in one cell only. Either the other cells are not yet differentiated or the amount of phosphate is too low to be detected. To obtain more detailed information about the extracellular matrix, a CH to phosphate ratio map is presented in Fig. 4: each pixel bearing a pseudo-color shows this ratio at a given position of the sample. We generated a line map crossing a cell to monitor the

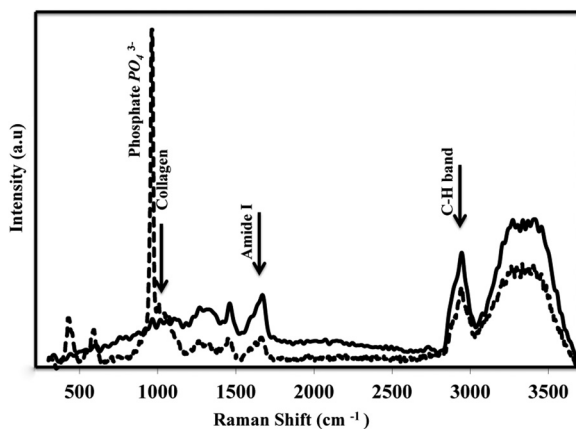


Fig. 2 The Raman spectra of individual cells in solid line and of the phosphate-rich region in dotted line.

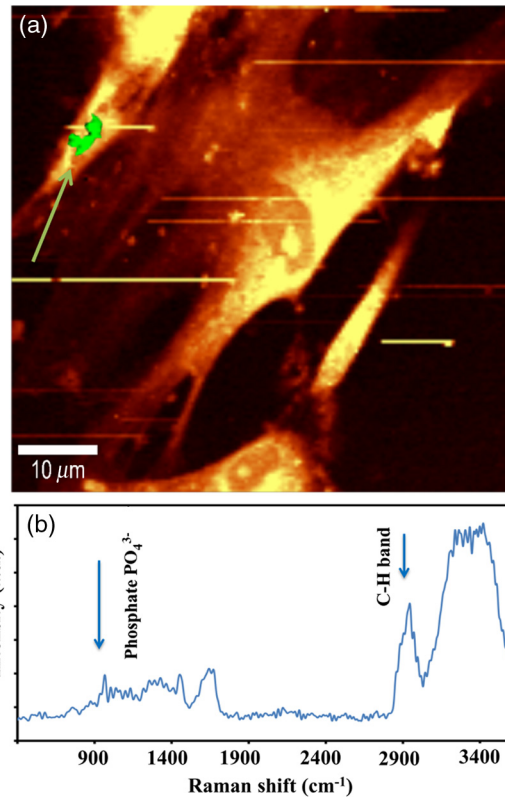


Fig. 3 (a) Reconstructed Raman image of cells obtained from CH stretching mode intensities (2800 to 3000 cm^{-1}). The green cluster presents the position of phosphate in the confocal plane of a single cell. (b) The average spectrum of the phosphate cluster is presented.

ratio: the red color at maximum corresponds to 30 times higher intensities of CH relative to that of phosphate. This ratio goes to the minimum when both ends of the line are out of the cell. The violet color belongs to the minimum ratio of CH relative to the phosphate intensities. Applying this method for a CH-to-phosphate ratio, false color chemical and line maps are provided. The advantage of calculating an organic matrix / mineral ratio map over the pure Raman spectra map is to provide fine details of the mineralized matrix around the differentiated cells. It also demonstrates that the Raman spectroscopy is a powerful instrument to measure the level of differentiation by detecting the intensity changes of mineral to organic components in DPSCs.

The most reported collagen band is amide I, as its components reveal changes in the collagen secondary structure. The ratio of two amide sub-bands is proportional to the relative amounts of trivalent cross-link pyridinoline and divalent cross-link dihydroxylysinonorleucine. Calculating the two amide I subpeaks' ratio provides precise information on the collagen cross-link and the matrix maturity. In order to monitor the collagen maturity that plays an important role in bone stiffness, we have measured collagen cross-linking by calculating the ratio of two amide I peak intensities (1660 and 1690 cm^{-1} , see spectra in Fig. 2). The two parts of the amide I mode are overlapped in one larger peak. A closer look at the spectrum reveals a shoulder on the amide band. To obtain a Raman image of a selected area on the sample, the number of pixels is first chosen considering the spatial resolution. For example, on an area of $100\text{ }\mu\text{m} \times 100\text{ }\mu\text{m}$, 150 lines are chosen and on each line 150 points are marked; therefore, 22,500 spectra (or pixels) are collected. Using the Witec Software, spectral images can

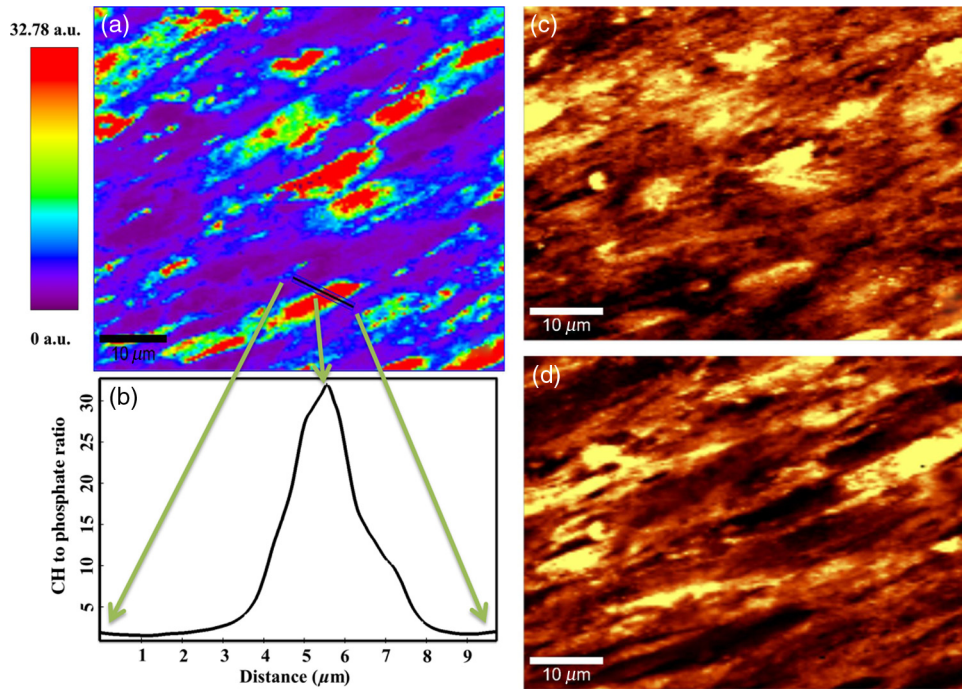


Fig. 4 (a) CH to phosphate ratio map; the red color presents the maximum ratio and the violet the minimum. (b) A dark solid line crossing a cell is traced and the graph representing the variation of the CH/phosphate ratio over the line is plotted. (c) Reconstructed Raman image of cells obtained from CH stretching mode intensities (2800 to 3000 cm^{-1}). (d) Reconstructed Raman image of phosphate obtained from phosphate peak ($\nu_1\text{ PO}_4^{3-}$ first stretching mode) at 960 cm^{-1} .

be reconstructed choosing a specific peak (e.g., CH image or phosphate image). To achieve a collagen maturity image, we first plot the reconstructed Raman images for the two selected peaks in the amide I band (1660 and 1690 cm^{-1}); then we divide the two reconstructed images using Witec Plus software. Each

pixel in the image is represented by a false color in Fig. 5, which shows the intensity of the selected peak (e.g., red spots show the maximum intensity for the collagen cross-link). The vertical bar next to the images defines the look-up table. Red spots show the highest Raman signal coming from the cross-linked collagen.

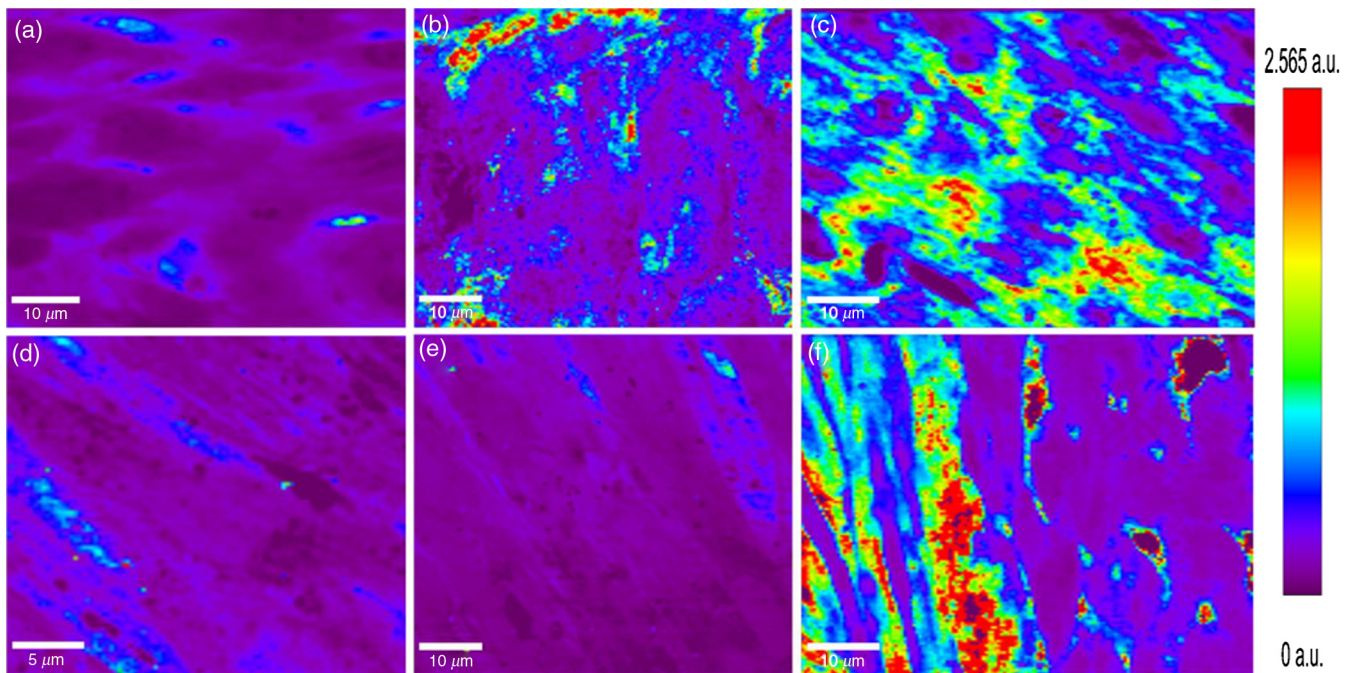


Fig. 5 (a) to (c) Collagen cross-link of the cells cultured in the osteogenic medium (days 7, 14, and 21). (d) to (f) Collagen cross-link of the cells cultured without the osteogenic medium (days 7, 14, and 21). The scale bar is $10\text{ }\mu\text{m}$ [except in (d), $5\text{ }\mu\text{m}$].

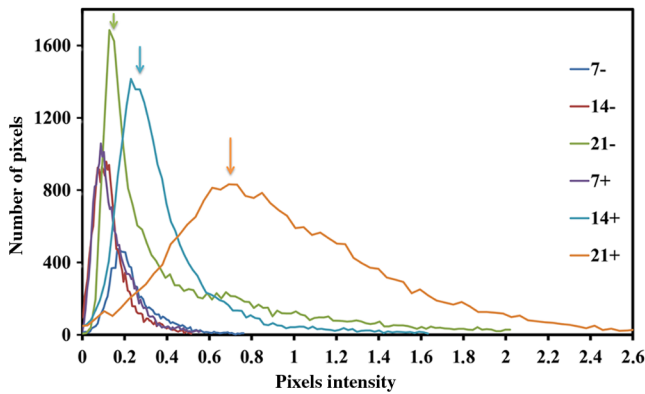


Fig. 6 Pixels' intensity histogram. Each graph presents the pixel intensities' distribution for the corresponding image in Fig. 5 for cells cultured for 7, 14, and 21 days. The signs + and - indicate the data for cells cultured in the osteogenic medium and without the osteogenic medium, respectively. The horizontal axis "Pixels' intensity" indicates the collagen cross-link index corresponding to cells presented in Fig. 5.

Figure 5 presents two sets of images obtained for cells cultured in osteogenic medium (days 7, 14, and 21) [Figs. 5(a)–5(c)] and without osteogenic medium (days 7, 14, and 21) [Figs. 5(d)–5(f)]. As observed in Fig. 5(a), no significant collagen cross-linking is observed after seven days of cell culture. Collagen cross-linking appears after 14 days culture in the osteogenic medium [Fig. 5(b)]; this becomes even more accentuated after 21 days [Fig. 5(c)]. The bottom line in Figs. 5(d)–5(f) shows that at 7, 14, and 21 days, cell cultivation without osteogenic medium collagen cross-linking is retarded: collagen cross-linking is observed after 21 days only [Fig. 5(f)]. Comparing the images in Fig. 5, it is obvious that cultures at day 21 (both with and without osteogenic medium) show the highest collagen cross-linking.

The image presenting collagen cross-linking seems to indicate a possible relationship between collagen cross-linking and the presence of the osteogenic medium. For a more accurate statistical evaluation, a pixel intensity histogram was plotted (Fig. 6). This histogram shows the number of pixels with a specific intensity indicating the collagen cross-link index corresponding to cells presented in Fig. 5. The orange histogram belongs to the 21-day cell culture in the osteogenic medium and has the highest intensity ratios (e.g., 400 pixels with collagen cross-linking ratio of 1.4). Briefly, by plotting the histogram in Fig. 6, the numbers of pixels (frequency) with a specific intensity in the function of the pixel intensities are provided, data that are not readable with this accuracy in the ratio map in Fig. 5. The arrows show the positions of the three largest histograms bearing the highest numbers of pixels. For cells cultured 21 days in the presence of the osteogenic medium, the maximum collagen cross-link index is ~ 0.7 (a.u.), while after 14 days in the osteogenic medium, this index decreases to ~ 0.2 (a.u.). The third best result (~ 0.12 a.u.) was obtained for cells cultured for 21 days without the osteogenic medium. Considering the area defined by the number and intensity of pixels represented in Fig. 6, we found that the histograms corresponding to day 21+ cultures contain more spectra of cross-linked collagen. The second and third highest collagen cross-linking appears at day 14 culture with the osteogenic medium and at day 21 without the osteogenic medium, respectively.

4 Discussion

In this study, we applied confocal Raman microscopy to evaluate the differentiation of DPSCs into osteoblasts and the maturity of the produced collagen fibers. The cultured cells with and without the osteogenic medium were imaged each seventh day until day 21. The cells cultured in osteogenic medium produce phosphate after 21 days. The vibrational mode at 960 cm^{-1} is chosen to construct a Raman map of the phosphate that is then compared with the cells' map obtained using CH bands (2800 to 3000 cm^{-1} for lipids, proteins, and carbohydrates). The results enable localization of phosphate around the cells, indicating the differentiation of DPSCs into osteoblast-like cells. Cells cultured without osteogenic medium showed no phosphate sign at any day from 0 to 21. In long-term culture and in the presence of the osteogenic medium, cells are confluent, form multilayers, and hence the phosphate signal recorded around these cells is accompanied with the CH peaks of other cell layers. Collagen cross-linking during differentiation of DPSCs was monitored by calculating the ratio of two amide I peaks at 1660 and 1690 cm^{-1} . Maximum cross-linking of collagen is observed after 21 days' cell culture in both the absence and presence of the osteogenic medium, though the osteogenic medium is needed to produce collagen at early cell culture periods.

5 Conclusion

Confocal Raman microscopy is applied to monitor DPSCs differentiation into osteoblast-like cells and maturation of extracellular matrix. We first isolate, in the measured Raman spectra, the phosphate peaks and the CH bands to provide a detailed map of phosphate produced by the cells, indicating their differentiation into osteoblasts after three weeks of culturing in the presence of the osteogenic medium. By plotting the CH/phosphate signal ratio, a detailed analysis is provided. Calculating the ratio of two amide peaks, we monitor the collagen cross-linking in cell cultures after 21 days. Our work demonstrates that confocal Raman microscopy is a powerful label-free and noninvasive imaging technique to monitor the process of cell differentiation, providing valuable insight in the organic/inorganic composition of cell cultures over long time scales (up to three weeks). However, to obtain more information, appropriate data analysis methods should be applied to the measured raw Raman spectra. Here, we trace for the first time, stem cells' differentiation and the formation of a mature organic matrix, pointing toward promising applications of DPSCs for tissue engineering.

References

1. A. Arthur, A. Zannettino, and S. Gronthos, "The therapeutic applications of multipotential mesenchymal/stromal stem cells in skeletal tissue repair," *J. Cell. Physiol.* **218**, 237–245 (2009).
2. T. Ma, "Mesenchymal stem cells: from bench to bedside," *World J. Stem Cells* **2**(2), 13–17 (2010).
3. R. d'Aquino et al., "Human postnatal dental pulp cells co-differentiate into osteoblasts and endothelialocytes: a pivotal synergy leading to adult bone tissue formation," *Cell Death Differ.* **14**(6), 1162–1171 (2007).
4. S. Gronthos et al., "Postnatal human dental pulp stem cells (DPSCs) in vitro and in vivo," *Proc. Natl. Acad. Sci.* **97**(25), 13625–13630 (2000).
5. N. M. B. K. Willems et al., "Determination of the relationship between collagen cross-links and the bone-tissue stiffness in the porcine mandibular condyle," *J. Biomech.* **44**, 1132–1136 (2011).
6. M. M. Mariani, P. J. Day, and V. Deckert, "Applications of modern micro-Raman spectroscopy for cell analyses," *Integr. Biol.* **2**, 94–101 (2010).

7. K. E. Shafer-Peltier et al., "Model-based biological Raman spectral imaging," *J. Cell. Biochem.* **87**, 125–137 (2002).
8. C. Krafft, B. Dietzek, and J. Popp, "Raman and CARS microspectroscopy of cells and tissues," *Analyst* **134**, 1046–1057 (2009).
9. K. Hartmann et al., "A study of Docetaxel-induced effects in MCF-7 cells by means of Raman microspectroscopy," *Anal. Bioanal. Chem.* **403**, 745–753 (2012).
10. H. K. Chiang et al., "In situ Raman spectroscopic monitoring of hydroxyapatite as human mesenchymal stem cells differentiate into osteoblasts," *J. Raman Spectrosc.* **40**, 546–549 (2008).
11. C. Matthäus et al., "Label-free detection of mitochondrial distribution in cells by nonresonant Raman microspectroscopy," *Biophys. J.* **93**, 668–673 (2007).
12. M. Dominici et al., "Minimal criteria for defining multipotent mesenchymal stromal cells. The International Society for Cellular Therapy position statement," *Cytotherapy* **8**(4), 315–317 (2006).
13. C. Coppe, Y. Zhang, and P. K. Den Besten, "Characterization of primary dental pulp cells in vitro," *Pediatr. Dent.* **31**(7), 467–471 (2009).
14. S. Shi and S. Gronthos, "Perivascular niche of postnatal mesenchymal stem cells in human bone marrow and dental pulp," *J. Bone Miner. Res.* **18**(4), 696–704 (2003).
15. P. Kémoun et al., "Human dental follicle cells acquire cementoblast features under stimulation by BMP-2/-7 and enamel matrix derivatives (EMD) in vitro," *Cell Tissue Res.* **329**(2), 283–294 (2007).
16. H. Salehi et al., "Confocal Raman data analysis enables identifying apoptosis of MCF-7 cells caused by anticancer drug paclitaxel," *J. Biomed. Opt.* **18**(5), 056010 (2013).
17. Z. Huang et al., "Near infrared Raman microscopy for optical diagnosis of lung cancer," *Int. J. Cancer* **107**, 1047–1052 (2003).

Hamideh Salehi received her PhD in biophysics from the University of Montpellier, and she was a postdoctoral researcher in biomedical engineering at the University of California, Irvine. She has obtained

her master's degrees in physics, photonic crystals, and mechanical engineering. Her research interests are cancer therapy with stem cells and the study of living cells treated with drugs and nanoparticles by confocal Raman microscopy and stimulated Raman spectroscopy. She also collaborated with biofilm and dental research groups.

Pierre-Yves Collart-Dutilleul received his PhD degree in 2013 at Montpellier University in the BioNano Laboratory under the supervision of professor Frédéric Cuisinier. After completion of his degree of doctor in dental surgery in 2006, he got a master's degree in cell biology and then a PhD in tissue engineering. His research focuses on dental pulp stem cells adhesion, proliferation, and osteodifferentiation on porous scaffolds, for orthopedic tissue engineering and drug delivery applications.

Csilla Gergely received her PhD in biophysics, Szeged University. She is professor in Charles Coulomb Laboratory of the Montpellier University and head of the bionanophotonics team. Her research interests lie in elaborating adhesion peptides for selective biofunctionalization of photonic crystals for elaboration of semiconductors based biosensing, and developing various microscopic techniques (near-probe and multiphoton microscopy) for functional imaging and follow-up therapy of cancerous cells. She has authored 85 peer-reviewed articles and book chapters.

Frédéric J. G. Cuisinier received his PhD in 1989 at Strasbourg University under the direction of professor Robert Franck and is a professor in dentistry. He authored more than 120 papers on high-resolution electron microscopy of mineralized tissues, biomineralization, biosensors, and multilayer film build-up. His current research concerns confocal Raman microscopy of living cells, multiphotonic microscopy of dental tissue, and biomaterial interactions with dental pulp stem cells.